

## Optical and magneto-optical response of a doped Mott insulator

M. S. Laad,<sup>1</sup> L. Craco,<sup>2</sup> and E. Müller-Hartmann<sup>1</sup>

<sup>1</sup>*Institut fuer Theoretische Physik, Universitaet zu Koeln, Zuelpicher Strasse, 50937 Koeln, Germany*

<sup>2</sup>*Instituto de Física Gleb Wataghin - UNICAMP, C.P. 6165, 13083-970 Campinas - São Paulo, Brazil*

(Received 24 August 2000; published 26 July 2001)

We study the optical, Raman, and ac Hall response of the doped Mott insulator within the dynamical mean-field theory ( $d=\infty$ ) for strongly correlated electron systems. The occurrence of the *isosbectic* point in the optical conductivity is shown to be associated with the frequency dependence of the generalized charge susceptibility. We compute the Raman response, which probes the fluctuations of the “stress tensor,” and show that the scattering is characterized by appreciable incoherent contributions. The calculated ac Hall constant and Hall angle also exhibit the isosbectic points. These results are also compared with those obtained for a *non-FL* metal in  $d=\infty$ . The role of low-energy coherence (FL) or incoherence (non-FL) in determining the finite frequency response of strongly correlated metals in  $d=\infty$  is discussed in detail. As an application of interest, we compute the dielectric figure-of-merit (DFOM), a quantity that is of potential importance for microwave device applications. We demonstrate explicitly that systems near the filling driven Mott transition might be good candidates in this respect, and discuss the influence of real-life factors on the DFOM.

DOI: 10.1103/PhysRevB.64.075108

PACS number(s): 75.30.Mb, 74.80.-g, 71.55.Jv

The celebrated Landau theory of the Fermi liquid (FL),<sup>1</sup> has been the mainstay of the conventional theory of metals for over four decades. It has proved to be remarkably stable even when local correlations are strong, as has been observed in a variety of heavy fermion metals. Recent theoretical work concentrating on the  $d=\infty$  limit of lattice fermionic models has shown up the robustness of the local Fermi-liquid picture, even for large values of the interaction.<sup>2</sup>

The  $d=\infty$  works have also clarified the conditions under which the metallic phase for a given lattice model is described by FL theory;<sup>3</sup> in the situation where symmetry breaking is suppressed, the FL metal survives as long as there is no ground-state degeneracy, as in the Hubbard model. In every case where the ground state exhibits a degeneracy as a function of the model parameters, FL behavior is invalidated; examples are the quantum paramagnetic phases of the spinless Falicov-Kimball model<sup>4</sup> and the two-channel Kondo model<sup>5</sup> in this limit. The crucial role of the transfer of spectral weight over wide-energy scales across the insulator-metal transition has also been revealed; it has thereby become clear that the itinerant and the atomic aspects of the problem should be treated consistently on a common footing to obtain reliable answers.

Optical conductivity is an insightful probe that can provide detailed information about the finite frequency charge dynamics of a correlated electronic fluid.<sup>6</sup> In recent years, much information about the non-Fermi liquid charge dynamics in the “normal” state of cuprate superconductors has been gleaned by careful optical measurements.<sup>6</sup> The in-plane optical conductivity,  $\sigma_{ab}(\omega)$  for hole-doped cuprates shows a non-FL fall off with  $\omega$  at small  $\omega \ll D$  ( $D$  is the bandwidth),<sup>6</sup> while the electron-doped cuprate  $\text{Nd}_{2-x}\text{Ce}_x\text{CuO}_{4-y}$  shows behavior characteristic of a FL.<sup>6</sup> A curious feature observed in these studies is the fact that the various  $\sigma_{ab}(\omega)$  curves for different dopings cross at a *single* point (this is the *isosbectic* point in the literature). It is interesting to ask for the underlying physics manifesting itself in such observations.

Hall measurements provide a detailed picture of finite-frequency charge excitations in an external magnetic field, and probe the nature of the transverse-scattering processes in an electronic fluid.<sup>7</sup> Measurements carried out on the cuprates show that the transverse-scattering processes are characterized by anomalous temperature and frequency dependences, leading to the two-relaxation rate phenomenology.<sup>7</sup> It is well known that FL transport is generically characterized by a *single*-scattering rate governing transport, and the appearance of two-relaxation rates is therefore cited as a striking manifestation of the breakdown of FL ideas.

Given the above, the theoretical problem of computing the ac conductivity tensor for a strongly correlated metal is interesting; this quantity encodes detailed information about the finite-frequency charge excitations and their response to external electric and magnetic fields. Theoretically, the problem of computing the transport coefficients for a strongly correlated fermionic system in a controlled way is a rather hard task. The problem is even harder in the case of magnetotransport; to compute the Hall conductivity tensor, one has to evaluate explicitly three-point functions. In finite-spatial dimensions, vertex corrections, which may be important, cannot be evaluated satisfactorily in any controlled approximation. The above difficulties make it imperative to search for controlled approximation schemes where some of the above difficulties can be circumvented without sacrificing essential correlation effects.

The dynamical mean-field approximation (DMFA or  $d=\infty$ ) has proved to be a successful tool to investigate transport in strongly correlated systems in a controlled way.<sup>8</sup> This is because the vertex corrections entering in the Bethe-Salpeter equation for the two-particle propagator for the conductivity vanish rigorously in  $d=\infty$ . To evaluate the conductivity tensor, one needs only to compute the fully interacting *local* self-energy of the given model, following which the Kubo formalism can be employed.<sup>9</sup> Given that DMFA captures the nontrivial local dynamics exactly, one expects that it provides an adequate physical description in situations

where local fluctuations are dominant. In fact, the dc resistivity and Hall effect, as well as the longitudinal ac conductivity for the Hubbard model, have already been considered in the literature, in the framework of the  $d=\infty$  approximation.<sup>10</sup>

However, the harder problem of computing the frequency-dependent Hall effect (Hall constant and angle) has not been studied to date in detail. Actually, Lange<sup>7</sup> has employed the Mori-Zwanzig projection formalism to study dc magnetotransport in the Hubbard model. The actual evaluation of the complicated equations is, however, actually carried out in the Hubbard I approximation. This is known to lead to spurious instabilities (like ferromagnetism, which is washed away when local quantum fluctuations are included). Moreover, only the dc Hall constant is evaluated explicitly. The Hubbard I approximation does not correctly capture the transfer of high-energy spectral weight to low energy upon hole doping, a feature characteristic of correlated systems, and so one expects that it will be inadequate when one attempts to look at the ac conductivity. Some of the deficiencies of the Hubbard I approximation may be cured by the so-called Hubbard III approximation;<sup>12</sup> this is actually the exact solution of the  $d=\infty$  Falicov-Kimball model.<sup>13</sup> However, the metallic phase is not a Fermi liquid, and actually describes the charge dynamics in a model with x-ray edge singularities at low energy.<sup>4</sup> More recently, Lange<sup>7</sup> have computed the ac Hall constant using the iterated perturbation theory (IPT) in  $d=\infty$ . However, the ac Hall angle and the Raman response, which we compute, has not been considered in Ref. 7. Additionally, we have also compared our results with those obtained for a non-FL metal<sup>12</sup> in  $d=\infty$  to clarify the role of low-energy coherence (incoherence) in determining the ac response of correlated metals. The detailed doping and frequency dependence of the Hall constant and Hall angle for a strongly correlated FL in  $d=\infty$  thus remains an open problem to date.

In this paper, we attempt to fill in this gap by studying the ac Hall effect and its doping dependence in detail. We concentrate on the one-band Hubbard model; the simplest model exhibiting FL behavior in  $d=\infty$ . We have recently studied the ac Hall response for the ‘‘simplified Hubbard model’’<sup>12</sup> exactly in this limit, as mentioned above, it describes the response of a non-FL metal. We make an in-depth study of all the properties that can be computed without making further approximations. Specifically, we study the optical conductivity tensor, the ac Hall constant and Hall angle, as well as the Raman intensity line shape as a function of filling for the correlated FL metal. We also compare our results with those obtained for a non-FL metal in  $d=\infty$ . Lastly, as a specific application of the treatment presented here, we report the dielectric figure-of-merit (DFOM) in the strongly correlated metal. We show that systems near the filling-driven Mott transition might be good candidates for potential microwave device applications (high DFOM), and assess the role of real-life factors in optimizing the DFOM.

We start with the one-band Hubbard model,

$$H = -t \sum_{\langle ij \rangle, \sigma} (c_{i\sigma}^\dagger c_{j\sigma} + \text{H.c.}) + U \sum_i n_{i\uparrow} n_{i\downarrow}, \quad (1)$$

defined on a hypercubic lattice in  $d$  dimensions. In the  $d \rightarrow \infty$  limit, this corresponds to a Gaussian unperturbed density of states (DOS).<sup>2</sup> In this limit, the lattice model, Eq. (1), is mapped onto a one-channel Anderson impurity problem (SIAM) embedded self-consistently in a dynamical ‘‘bath’’ function that encodes the dynamical information about the quantum nature of the problem. Solution of the HM [Eq. (1)] therefore requires a reliable way to solve the impurity problem.<sup>2</sup> Unfortunately, there is no exact analytical solution available for the SIAM, and one has to resort to schemes that give reliable answers, and agree well with ‘‘exact’’ methods, e.g., with exact diagonalization.<sup>2</sup> In this paper, we use the iterated perturbation theory (IPT) away from half filling<sup>14</sup> to solve the SIAM. This technique uses the Friedel sum rule<sup>15</sup> (equivalent to the Luttinger theorem) to ensure that the correct Fermi-liquid behavior is recovered at low energy. By construction, it is also exact in the band and the atomic limits, and so is a reliable interpolation scheme that describes the *full* local dynamical spectrum for all  $U/t$  and band fillings. The inability of the IPT to treat broken-symmetry phases is not a serious problem here, since we restrict ourselves to study the ac response across the Mott transition. Knowledge of the local dynamics in the SIAM enables us to compute the full local dynamics of the HM in  $d=\infty$ . We do not repeat the features of this method here, but refer the interested reader to Ref. 14 for details.

Solution of the  $d=\infty$  problem using the IPT yields the *full* local self-energy  $\Sigma(\omega)$  and the Green function  $G(\omega) = 1/N \sum_{\mathbf{k}} G(\mathbf{k}, \omega) = 1/N \sum_{\mathbf{k}} [\omega - \epsilon_{\mathbf{k}} - \Sigma(\omega)]^{-1}$  for the symmetry unbroken paramagnetic case, which we consider here. We have computed the local DOS for the HM, and have checked that all features of the strongly correlated Fermi-liquid metal are reproduced in accordance with (Ref. 14). The quadratic energy dependence of  $\text{Im}\Sigma(\omega)$  at small energy, the collective Fermi liquid peak that shifts to lower energy with hole doping, as well as the transfer of spectral weight from the upper to the (central FL resonance + lower) Hubbard band are all reproduced well.

As mentioned above, knowledge of  $\Sigma(\omega)$  for the lattice problem is the only input required to calculate the optical conductivity tensor in  $d=\infty$ . Since vertex corrections drop out in the two-particle equation for the conductivity in this limit, the longitudinal optical conductivity is given by a simple bubble diagram involving the *full* interacting, local propagators. Using the well-known equation for  $\sigma_{xx}(\omega)$ ,<sup>2,16</sup>

$$\sigma_{xx}(i\omega) = \frac{1}{i\omega} \int \rho_0(\epsilon) \sum_{i\nu} G(\epsilon, i\nu) G(\epsilon, i\omega + i\nu), \quad (2)$$

we have computed  $\sigma_{xx}(\omega)$  for a given choice  $U/D=3.0$  and for different band fillings  $\delta=(1-n)$  ( $D$  is the effective bandwidth of the noninteracting model). The results are shown in Fig. 1. We see that  $\sigma_{xx}(\omega)$  shows three distinct features worthy of mention: (1) The low-energy part ( $\omega < 0.25$ ) is characteristic of a renormalized FL metal, and correlates well with the behavior of the central FL peak in the DOS. (2) However,  $\sigma_{xx}(\omega)$  begins to rise again around  $\omega/D \approx 1$ , passes through a broad peak centered around  $U/2$  (for  $n=1$ ), and starts falling off at larger frequencies. The

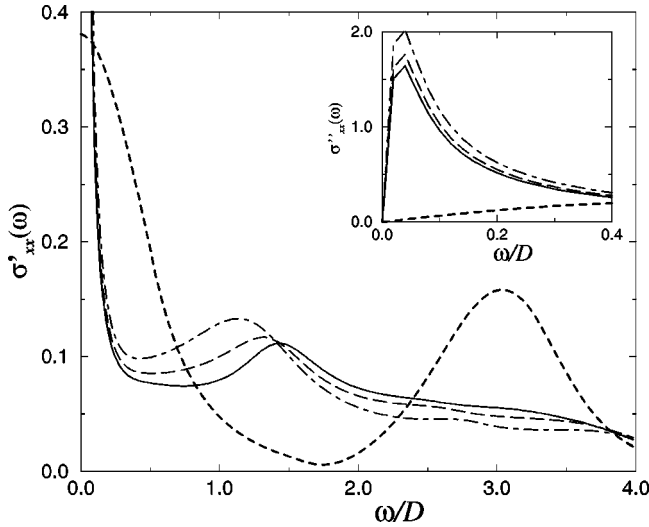


FIG. 1. The optical conductivity of the Hubbard model with  $U/D=3.0$  for various band fillings;  $\delta=0.1$  (solid line),  $\delta=0.2$  (dashed line),  $\delta=0.3$  (dot-dashed line).  $\sigma_{xx}(\omega)$  for the FKM (non-FL) for  $U/D=3.0$  and  $\delta=0.1$  (bold-dashed line).

transfer of optical spectral weight from high- to low-energy upon hole doping is clearly exhibited, and is understandable in terms of the interplay between the high-energy (localized) part, which inhibits double occupancies, and the low-energy (coherent) part of the spectrum, reflecting carrier itinerancy that increases with hole doping. (3) Most interestingly, the  $\sigma_{xx}(\omega)$  curves for various  $\delta$  all cross at a *single* point ( $\omega \approx 1.4D$ ); this is the *isosbestic* point cited in earlier work.<sup>4</sup> These are exactly the features observed in optical experiments performed on  $\text{Nd}_{2-x}\text{Ce}_x\text{CuO}_{4-y}$ ,<sup>6</sup> which shows FL behavior in contrast to the hole-doped cuprates. We have a partial understanding of this curious feature: Following Vollhardt,<sup>18</sup> who investigated such features seen in the specific heat for the HM for different  $U$ , we ask for the reasons for the crossing of the different curves, and the width of the crossing region. Focusing on the first part of the question, it is easy to show that there must exist some  $\omega = \omega_c(n)$  for which the curves cross. First, consider the high-energy limit of our results. In general,  $\sigma_{xx}(\omega) = -\chi''(\omega)/\omega$ . Now, as  $\omega \rightarrow \infty$ ,  $\Sigma(\omega) = U^2(n/2)(1-n/2)/\omega$ , and  $G(\omega) = 1/\omega$ , so that  $\sigma_{xx}(\omega \rightarrow \infty) = (n/2)(1-n/2)/\omega$ , whereby  $d\sigma_{xx}/dn > 0$  for  $\omega \rightarrow \infty$  for all  $n < 1$ . On the other hand, it is clear from Fig. 1, as well as from the optical sum rule, that  $\sigma_{xx}(\omega)$  *increases* with increasing  $\delta$ , i.e., with *decreasing*  $n$ , at energies  $\omega \leq 1.4D$ , so that we have  $d\sigma_{xx}/dn < 0$  at small  $\omega$ . This implies that  $\sigma_{xx}(\omega)$  curves for different  $\delta$  must cross at some  $\omega_c(n)$ . This crossing occurs at a single point if  $\omega_c(n)$  is independent of  $n$ . Our results show that this seems to be the case to a high accuracy, but we are unable to quantify this argument further. It is an interesting problem to inquire into the deeper reasons for such features in the HM [see Ref. 18 for a thorough discussion of the crossing points in  $C_p(U, T)$ ].

Knowledge of the longitudinal optical conductivity allows us to compute the Raman spectrum within the  $d=\infty$  methodology. This is because, as long as  $\sigma_{xx}(\omega)$  is completely determined by the renormalized bubble contribution (vertex

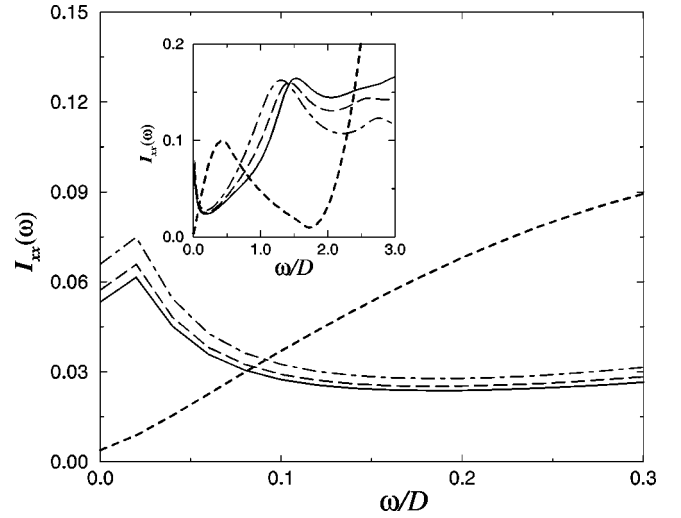


FIG. 2. Raman intensity line shape  $I_{xx}(\omega)$  for the Hubbard model (FL) with  $U/D=3.0$ , and for various band fillings;  $\delta=0.1$  (solid line),  $\delta=0.2$  (dashed line),  $\delta=0.3$  (dot-dashed line).  $I_{xx}(\omega)$  for the FKM (non-FL) for  $U/D=3.0$  and  $\delta=0.1$  (bold-dashed line).

corrections drop out, as in  $d=\infty$ ), the Raman intensity is directly related to the optical conductivity<sup>19</sup> via the equation,

$$I_{xx}(\omega) = \frac{\omega}{1 - e^{-\beta\omega}} \text{Re } \sigma_{xx}(\omega). \quad (3)$$

In Fig. 2, we show the Raman line shapes calculated from Eq. (3) for the same  $U/D$  and doping values. Since all calculations are carried out at  $T=0.01$ ,  $I_{xx}(\omega)$  is finite at  $\omega = 0$ . A sharp peak at low energy, reminiscent of the plasmon peak in continuum treatments,<sup>19</sup> is visible, followed by an incoherent response characteristic of Mott-Hubbard systems<sup>19</sup> at higher energies. However, the low-energy peak is more the characteristic of the coherent part of the particle-hole response at low energies in a strongly correlated Fermi liquid. Evidence in favor of this interpretation is provided by the fact that the sharp peak broadens out as the temperature is raised above  $T_K$ , the lattice Kondo temperature, where it is destroyed by strong scattering off local moments (which exist for  $T > T_K$ , rendering the FL description invalid).

It is interesting to compare the above results with those obtained for a non-Fermi-liquid (NFL) metal in  $d=\infty$ . In this limit, NFL behavior at  $T=0$  is obtained when the local Kondo effect is suppressed; this is exactly what happens in the Falicov-Kimball model (FKM) in this limit.<sup>4</sup> Since the  $\downarrow$ -spin hopping is zero in the FKM, the Kondo effect does not occur, and the metallic state is not a FL near half filling [it is actually described by the local x-ray edge physics in  $d=\infty$  (Ref. 17)]. In the inset of Figs. 1–2, we show the real part of  $\sigma_{xx}(\omega)$  and the Raman intensity line shape for the FKM with identical values of  $U/D=3.0$  and hole doping ( $\delta=0.1$ ). It is seen that  $\sigma_{xx}(\omega)$  for the FKM falls off much more slowly (like  $1/\omega$ ) in comparison with the fast Drude-like falloff observed for the HM. As expected, the sharp low-energy peak in  $I_{xx}(\omega)$  is changed into a broad continuum, reflecting an incoherent low-energy response charac-

teristic of a NFL metal. We also observe that  $I_{xx}(\omega=0) \neq 0$  at  $T=0$  in the FKM case, as argued by Shastry and Shraiman.<sup>19</sup> This corresponds to the fact that, in a non-FL metal (where the Green function has a branch cut rather than a pole structure), the action of the kinetic energy, or the stress tensor [which has nonvanishing matrix elements between lower-Hubbard band (LHB) states] does not create well-defined elementary excitations. This results in the broad continuum with nonvanishing intensity in the FKM (NFL), in contrast to the sharp peak with vanishing intensity (at  $T=0$ ) in the HM (FL) observed above. Hence, the finite-frequency response of correlated metals is determined by the presence of a pole (branch cut) structure in the single-particle Green function at low energy. Within the  $d=\infty$  ideas used here, the low-energy coherence is a manifestation of the collective lattice Kondo effect in the Hubbard model, while the incoherent response in the non-FL case is understood in terms of the vanishing of the  $\downarrow$ -spin hopping, and to the complete suppression of this Kondo scale.

As mentioned above, computation of the magnetotransport is an extremely delicate matter, since one has to evaluate *three-point* functions<sup>7</sup> to first order in the external magnetic vector potential  $\mathbf{A}$ . Generally speaking, in a nearly free electron picture, the Hall effect is determined by the vagaries (shape and size) of the Fermi surface. That such a correspondence cannot be made for strongly correlated metals was pointed out by Shastry *et al.*<sup>20</sup> showed that the Hall constant in a strongly correlated system is dominated by spectral weight far from the Fermi surface, and hence, is independent of its shape. This suggests that the results should not be sensitive to the choice of the free DOS, allowing us to use the  $d=\infty$  DOS for the hypercubic lattice. Calculations for a three-dimensional (3D) system, where the  $d=\infty$  approach works quite well,<sup>2</sup> can be carried out by replacing the  $d=\infty$  DOS by a 3D DOS.

To compute the Hall conductivity, we need to add a Peierls coupling term to the HM, where it enters via the hopping.<sup>20</sup> The Hamiltonian in a magnetic field is

$$H = - \sum_{\langle ij \rangle, \sigma} t_{ij}(\mathbf{A}) (c_{i\sigma}^\dagger c_{j\sigma} + \text{H.c.}) + U \sum_i n_{i\uparrow} n_{i\downarrow}, \quad (4)$$

where the hopping matrix elements are modified by a Peierls phase factor and are  $t_{ij} = \exp(2i\pi/\phi_0 \int_i^j \mathbf{A} \cdot d\mathbf{l})$ , where  $\mathbf{A}$  is the vector potential and  $\phi_0 = \text{H.c.}/e$ . The off-diagonal part of the conductivity involves the computation of a *three-point* function to first order in the external field, as mentioned before. Fortunately, a convenient form has been derived by Lange,<sup>7</sup> and in this approach the imaginary part of  $\sigma_{xy}(\omega)$  is given by

$$\begin{aligned} \sigma_{xy}''(\omega) = & c_{xy} \int_{-\infty}^{+\infty} d\epsilon \rho_0(\epsilon) \epsilon \int_{-\infty}^{+\infty} d\omega_1 d\omega_2 A(\epsilon, \omega_1) A(\epsilon, \omega_2) \\ & \times \frac{1}{\omega} \left[ \frac{F(\epsilon, \omega_1; \omega) - F(\epsilon, \omega_2; \omega)}{\omega_1 - \omega_2} + (\omega \rightarrow -\omega) \right], \end{aligned} \quad (5)$$

where

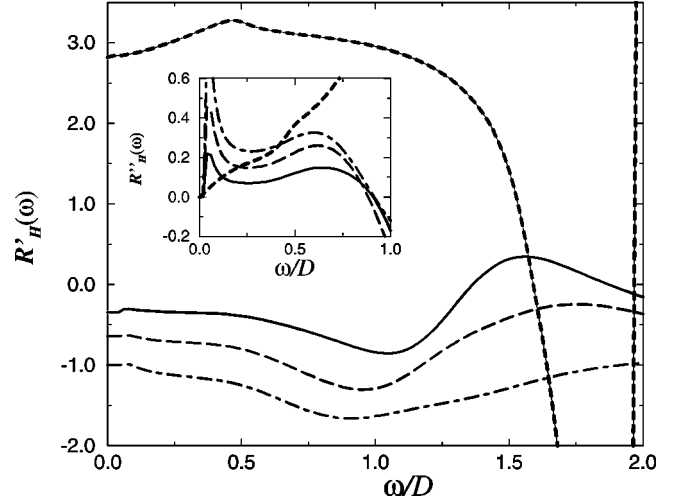


FIG. 3. AC Hall constant of the Hubbard model with  $U/D = 3.0$  for various band fillings;  $\delta=0.1$  (solid line),  $\delta=0.2$  (dashed line),  $\delta=0.3$  (dot-dashed line).  $\text{Re}R'_H(\omega)$  for the FKM (non-FL) for  $U/D=3.0$  and  $\delta=0.1$  (bold-dashed line).

$$F(\epsilon, \omega; \omega_1) = A(\epsilon, \omega_1 - \omega) [f(\omega_1) - f(\omega_1 - \omega)], \quad (6)$$

and  $A(\epsilon, \omega) = -\text{Im}[\omega - \epsilon - \Sigma(\omega)]^{-1}/\pi$  is the sp spectral function in  $d=\infty$ .

Given the sp spectral function in  $d=\infty$ ,  $\sigma_{xy}''(\omega)$  is computed from the above, and the corresponding real part is obtained from a Kramers-Krönig transform. The Hall constant and Hall angle are obtained directly as

$$R_H(\omega) = \frac{\sigma_{xy}(\omega)}{\sigma_{xx}^2(\omega)}, \quad (7)$$

and

$$\cot \theta_H(\omega) = \frac{\sigma_{xx}(\omega)}{\sigma_{xy}(\omega)}. \quad (8)$$

We describe the results obtained for the HM with  $U/D = 3.0$  and  $\delta=0.1, 0.2, 0.3$ . In Fig. 3, we show the real part of the ac Hall constant,  $R'_H(\omega)$ , with the corresponding imaginary part in the inset. Since we work at a small  $T=0.01$ , the  $\omega=0$  part of  $R'_H$  is finite and negative, in agreement with Ref. 10 ( $R'_H$  is identically zero at  $\omega=0$ ). At small frequency,  $R_H(\omega)$  shows features in good agreement with Ref. 11; i.e., it is constant at small  $\omega$  in accordance with what is expected of a Fermi liquid. Interestingly enough, the isosbetic behavior shown in the optical conductivity is also shown up in  $R_H''(\omega)$ . The real part of  $R_H(\omega)$  is negative at low energy, as expected for a correlated Fermi liquid. For  $\delta=0.1$  (small doping)  $R'_H(\omega)$  decreases monotonically up to  $\omega/D \approx 1.04$ , and thereafter starts to increase, becoming positive in agreement with the results of Lange and Kotliar.<sup>11</sup> As a function of doping  $R'_H(\omega)$  becomes more FL-like and the frequency dependence is also less pronounced. Indeed, for  $\omega/D < 2$ , the real part of the ac Hall constant does not change in sign and the positive peak observed in the low-doping limit at  $\omega/D \approx 1.5$  is totally suppressed for  $\delta=0.3$  (see Fig. 3 for more

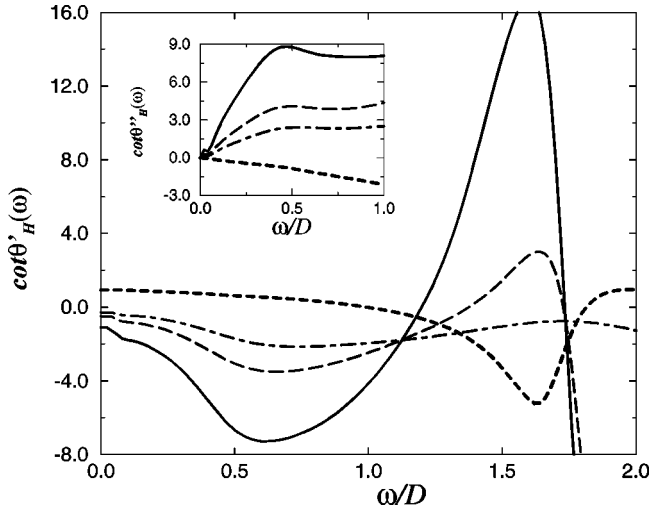


FIG. 4. AC Hall angle for the Hubbard model with  $U/D=3.0$  for various band fillings;  $\delta=0.1$  (solid line),  $\delta=0.2$  (dashed line),  $\delta=0.3$  (dot-dashed line).  $\cot \theta_H(\omega)$  for the FKM (non-FL) with  $U/D=3.0$  and  $\delta=0.1$  (bold-dashed line).

details). The corresponding results for the FKM (NFL) are shown with the bold-dashed line in Fig. 3. In this case  $R_H^r(\omega=0) > 0$ , in contrast to what is observed for the HM (FL), where it is negative. The underlying reason for this is again that in the FKM, the kinetic energy (stress tensor), which connects LHB states, does not create well-defined elementary excitations (since the Green function is totally incoherent).

In Fig. 4, we show the real and imaginary parts of the ac Hall angle computed from the above equation. First, we emphasize that we recover the correct Fermi-liquid form ( $\omega$ -independent) ac Hall angle at small  $\omega$ , in full agreement with Ref. 11. Furthermore, the strong frequency dependence of  $\cot \theta_H(\omega)$  found near half filling ( $\delta=0.1$ ) is weakened on increasing hole doping. The imaginary part is positive at low energy. This is again in marked contrast to the results of a similar calculation done for the NFL case (FK model), results for which are shown with the bold-dashed line in Fig. 4. We have also computed the frequency-dependent transverse scattering rate,  $\Gamma_{xy}(\omega)$  that goes like  $\omega^2$  in the case of the HM. In the case of the FKM,  $\Gamma_{xy}(\omega)$  goes like  $a\omega^2 + b$ , in marked contrast to the longitudinal relaxation rate, which follows a sublinear  $\omega$  dependence.<sup>9</sup> Since the transport-scattering rate as deduced from the Drude-like response of  $\sigma_{xx}(\omega)$  also varies quadratically in the  $d=\infty$  Hubbard model, the longitudinal- and transverse-scattering rates are described by a *single*-relaxation rate, as they should be in a FL metal. This is in contrast to the results obtained from a similar analysis for the FKM,<sup>12</sup> where the electron (hole)-like quasiparticles are absent, FL theory breaks down, and the longitudinal and transverse responses to an applied Lorentz field are governed by qualitatively different timescales.<sup>21–23</sup> In this context, it would be interesting to see whether the inclusion of short-ranged antiferromagnetic (AF) spin fluctuations (beyond  $d=\infty$ ) could push down the low-energy FL coherence scale in the  $d=\infty$  HM to zero, yielding a non-FL response. This is beyond the scope of the present

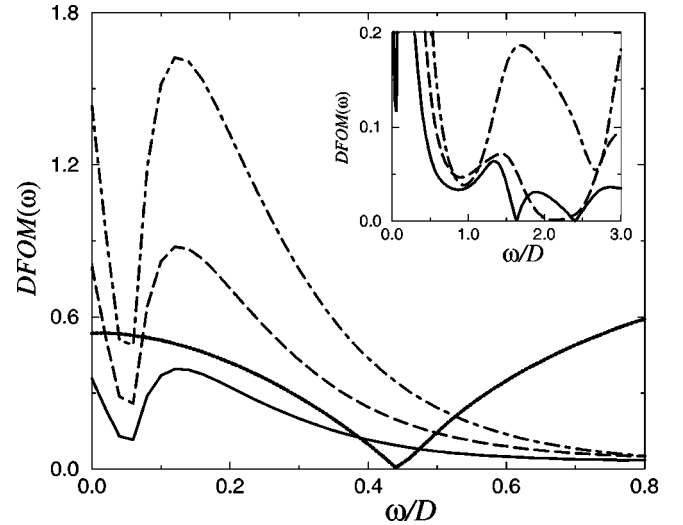


FIG. 5. The dielectric figure of merit [DFOM( $\omega$ )] for the Hubbard model with  $U/D=3.0$  for various band fillings;  $\delta=0.1$  (solid line),  $\delta=0.2$  (dashed line),  $\delta=0.3$  (dot-dashed line). DFOM( $\omega$ ) for the FKM (non-FL) for  $U/D=3.0$  and  $\delta=0.1$  (bold-dashed line).

paper, as no known controlled technique to access nonlocal vertex contributions (which enter into the Bethe-Salpeter equation for the conductivity in a nonlocal theory) is available.

Last, we present results for the dielectric figure of merit (DFOM) in the quantum paramagnetic metallic state as applications of the ideas presented above. The DFOM is a quantity that quantifies the dielectric efficiency of a material, and is of potential interest for microwave-device applications. A large value for the DFOM would make the material in question an attractive candidate for use in microwave-device applications. An attractive criterion in this context is the relation  $DFOM(\omega) > 1$ . Formally, the DFOM is defined as,

$$DFOM(\omega) = \frac{|\text{Im} \epsilon_{xy}(\omega)|}{2|\text{Im} \epsilon_{xx}(\omega)|}, \quad (9)$$

where  $\text{Im} \epsilon_{xy}(\omega)$  is the imaginary part of the off-diagonal dielectric constant. The above definition of the DFOM can be looked upon as the ac analogue of quantities like the thermoelectric figure of merit.<sup>24</sup> Thus, one requires the full dielectric tensor to access the DFOM. From the equation above, one sees that a high value for the DFOM depends on the detailed frequency dependences of the ac conductivity tensor. With specific reference to materials that undergo Mott transitions, one expects the DFOM to mirror the radical modification of the optical spectrum occurring across the transition. The Mott insulator is characterized by poor dielectric screening, while in the paramagnetic metal, dynamical screening should be effective. The dramatic transfer of optical spectral weight over large energy scales seen in the optical conductivity tensor should also be reflected in the DFOM. This fact might make such materials attractive candidates for potential device applications; a high DFOM in this context would be promising.

With this in mind, we show in Fig. 5 the results for the

DFOM calculated from the dielectric tensor. This is directly obtained from  $\sigma_{\alpha\beta}(\omega)$ ,  $\alpha, \beta = x, y$  via the equation  $\epsilon_{\alpha\beta}(\omega) = \delta_{\alpha\beta} + (4\pi/\omega)i\sigma_{\alpha\beta}(\omega)$ . The DFOM shows a strong peak at intermediate energy, and reaches values up to 1.6 for intermediate doping strength. This behavior is directly related to the minimum in  $\sigma_{xx}(\omega)$  [and hence in  $\text{Im}\epsilon_{xx}(\omega)$ ] around the energy range where the DFOM has a maximum. Since the features in  $\sigma_{xx}(\omega)$  are a direct consequence of the treatment of low- and high-energy features on an equal footing in the  $d=\infty$  Hubbard model, the high value of the DFOM at intermediate energies is also a direct fall out of the competition between the quasicohherent (low-energy) and incoherent (high-energy) processes characteristic of strongly correlated materials.

We believe that this number is an overestimate for real materials, since real band-structure effects, in conjunction with multiorbital situations and doping-induced static disorder, have the generic effect of reducing coherence in the metallic state, leading to smaller values of the DFOM. In real situations, multiorbital character of these materials, spin-orbit interactions, Jahn-Teller distortions, etc., have the effect of transferring optical spectral weight over large energy scales, and of pushing coherent low-energy spectral weight to high-energy (incoherent) regions. In principle, suitable extensions of the IPT technique used here for the single-band Hubbard model without disorder can be generalized to include these additional important effects without drastic conceptual difficulties. However, we believe that the DFOM will still have a respectable value when such effects are included, suggesting that materials close to filling-driven Mott transitions might be promising potential candidates for microwave-device applications.

An amusing feature of the present calculations done for the Hubbard model is the existence of isosbestic points in various calculated quantities, like  $\sigma'_{xx}(\omega)$ ,  $\text{Re}''_H(\omega)$ , and  $\cot\theta'_H(\omega)$ , as a function of hole doping (see Figs. 1–4). It is

an extremely interesting problem to examine this feature in more detail, perhaps in a manner analogous to Ref. 18. An interesting and open problem is to study multiorbital situations, which are more representative of the materials under consideration. We leave these issues for a more detailed investigation in the future.

In conclusion, we have determined the optical, Raman, and ac Hall response of the  $d=\infty$  Hubbard model using the IPT off half filling as a reliable approximation.<sup>14</sup> We have identified interesting features in the results (isosbestic points mentioned above), and shown that the response of a strongly correlated Fermi-liquid metal is explainable in terms of the competition between the atomic and itinerant aspects inherent in the Hubbard model. The evolution of the ac response with hole doping is controlled by the increasing weight of the quasicohherent processes (corresponding to transitions involving only the lower-Hubbard band states) relative to that of the high-energy incoherent features, whose weight diminishes with progressive hole doping. As an application of the ideas presented here, we have computed the dielectric figure of merit (DFOM), a number of importance in the context of possible microwave-device applications. Last, we have compared our results with those computed earlier by us for a non-FL metal in  $d=\infty$ , and have discussed the role of low-energy coherence (or incoherence) in determining finite-frequency response of strongly correlated metals. Given the success<sup>2</sup> of the  $d=\infty$  methodology in understanding aspects of the physics of three-dimensional transition-metal oxides, we believe that the calculation presented here in combination with the actual 3D band structure (which is equivalent to using the LDA DOS, for example) can be more relevant for studying ac response of 3D TM oxides.

One of us (M.S.L.) acknowledges financial support of SFB 341 of the German DFG. L.C. was supported by the Fundação de Amparo à Pesquisa do Estado de São Paulo (FAPESP).

<sup>1</sup>A.A. Abrikosov, L.P. Gorkov, and I.E. Dzyaloshinskii, in *Methods of Quantum Field Theory in Statistical Physics* (Pergamon, New York, 1963).  
<sup>2</sup>A. Georges *et al.*, Rev. Mod. Phys. **68**, 13 (1996).  
<sup>3</sup>A. Georges and G. Kotliar, Phys. Rev. B **45**, 6479 (1992).  
<sup>4</sup>A. Georges, G. Kotliar, and Q. Si, Int. J. Mod. Phys. B **6**, 705 (1992).  
<sup>5</sup>P. Nozieres and D. Pines, Phys. Rev. **109**, 741 (1958).  
<sup>6</sup>See, e.g., *High Temperature Superconductivity*, edited by D.M. Ginsberg (World Scientific, Singapore, 1990).  
<sup>7</sup>E. Lange, Phys. Rev. B **55**, 3907 (1997).  
<sup>8</sup>A. Khurana, Phys. Rev. Lett. **64**, 1990 (1990).  
<sup>9</sup>G. Möller, A.E. Ruckenstein, and S. Schmitt-Rink, Phys. Rev. B **46**, 7427 (1992).  
<sup>10</sup>P. Majumdar and H.R. Krishnamurthy, cond-mat/9512151 (unpublished).  
<sup>11</sup>E. Lange and G. Kotliar, Phys. Rev. Lett. **82**, 1317 (1999).  
<sup>12</sup>M.S. Laad and L. Craco, cond-mat/9806076 (unpublished).

<sup>13</sup>U. Brandt and C. Mielsch, Z. Phys. A **75**, 365 (1989); M.S. Laad, Phys. Rev. B **49**, 2327 (1994); L. Craco and M.A. Gusmão, *ibid.* **54**, 1629 (1996).  
<sup>14</sup>H. Kajueter and G. Kotliar, Phys. Rev. Lett. **77**, 131 (1996).  
<sup>15</sup>D.C. Langreth, Phys. Rev. **150**, 516 (1960).  
<sup>16</sup>See also, M. Jarrell *et al.*, Phys. Rev. B **51**, 11 704 (1995); M. Rozenberg *et al.*, *ibid.* **54**, 8452 (1996).  
<sup>17</sup>Q. Si, Phys. Rev. B **46**, 1261 (1992).  
<sup>18</sup>D. Vollhardt, Phys. Rev. Lett. **78**, 1307 (1997).  
<sup>19</sup>B.S. Shastry and B. Shraiman, Phys. Rev. Lett. **65**, 1068 (1990).  
<sup>20</sup>B.S. Shastry, B.I. Shraiman, and R.R.P. Singh, Phys. Rev. Lett. **70**, 2004 (1993).  
<sup>21</sup>H.D. Drew *et al.*, J. Phys.: Condens. Matter **8**, 10 037 (1996).  
<sup>22</sup>P.W. Anderson, in *The Theory of Superconductivity in the High- $T_c$  Cuprates* (Princeton University Press, Princeton, NJ, 1997).  
<sup>23</sup>Q. Si *et al.*, Int. J. Mod. Phys. B **6**, 705 (1992).  
<sup>24</sup>G. Palsson and G. Kotliar, Phys. Rev. Lett. **80**, 4775 (1998).